THE JOURNAL OF BIOLOGICAL CHEMISTRY
Vol. 277, No. 40, Issue of October 4, pp. 37663–37669, 2002

Printed in U.S.A.

Crystal Structure of a Laccase from the Fungus *Trametes versicolor* at 1.90-Å Resolution Containing a Full Complement of Coppers*

Received for publication, May 9, 2002, and in revised form, July 16, 2002
Published, JBC Papers in Press, August 5, 2002, DOI 10.1074/jbc.M204571200

Klaus Piontek‡, Matteo Antorini§, and Thomas Choinowski

From the Institute of Biochemistry, Swiss Federal Institute of Technology (ETH), ETH-Hönggerberg, Building HPM, Room D 8.1-2, CH-8093 Zürich, Switzerland

Laccase is a polyphenol oxidase, which belongs to the family of blue multicopper oxidases. These enzymes catalyze the one-electron oxidation of four reducing-substrate molecules concomitant with the four-electron reduction of molecular oxygen to water. Laccases oxidize a broad range of substrates, preferably phenolic compounds. In the presence of mediators, fungal laccases exhibit an enlarged substrate range and are then able to oxidize compounds with a redox potential exceeding their own. Until now, only one crystal structure of a laccase in an inactive, type-2 copper-depleted form has been reported. We present here the first crystal structure of an active laccase containing a full complement of coppers, the complete polypeptide chain together with seven carbohydrate moieties. Despite the presence of all coppers in the new structure, the folds of the two laccases are quite similar. The coordination of the type-3 coppers, however, is distinctly different. The geometry of the trinuclear copper cluster in the *Trametes versicolor* laccase is similar to that found in the ascorbate oxidase and that of mammalian ceruloplasmin structures, suggesting a common reaction mechanism for the copper oxidation and the O_2 reduction. In contrast to most blue copper proteins, the type-1 copper in the *T. versicolor* laccase has no axial ligand and is only 3-fold coordinated. Previously, a modest elevation of the redox potential was attributed to the lack of an axial ligand. Based on the present structural data and sequence comparisons, a mechanism is presented to explain how laccases could tune their redox potential by as much as 200 mV.

Among the few enzymes that are able to catalyze the four-electron reduction of molecular oxygen to water are the members of the blue multicopper oxidase (bmCuO)[1] family (for a review, see Ref. 1). The most prominent representatives of this family comprise laccase, ascorbate oxidase (AO), and mammalian plasma ceruloplasmin, which have been the subject of intensive investigations for many decades. The reduction of molecular oxygen is accompanied by a one-electron oxidation of reducing substrates. Blue copper oxidases contain at least one type-1 (T1) copper, which is presumably the primary oxidation site. Blue multicopper oxidases typically employ at least three additional coppers: one type-2 (T2) and two type-3 (T3) coppers arranged in a trinuclear cluster, the latter being the site at which the reduction of molecular oxygen takes place. The three different copper types can be differentiated from their spectroscopic behavior. The T1 copper has a strong absorption around 600 nm, which gives rise to the typical blue color of the copper oxidases. The T2, or "normal," copper exhibits only weak absorption in the visible region but is EPR-active, whereas the two coppers of the T3 site are characterized by an absorption band at about 330 nm. They are, however, EPR-silent due to an antiferromagnetic coupling mediated by a bridging ligand.

Laccase (benzenediol oxygen oxidoreductase, EC 1.10.3.2), a phenol oxidase with a molecular mass of about 70 kDa, catalyzes the oxidation of a broad range of substrates such as polyphenols, methoxy-substituted phenols, diamines, and some inorganic compounds (2–4). Since their discovery more than one century ago in the Japanese tree *Rhus venicifera* (5), laccases have been found to be widely distributed among plants, where they are involved in the wounding response and the synthesis of lignin. Lignin, which provides the structural component of the plant cell wall, is a heterogeneous and complex biopolymer that consists of phenyl propanoid units linked by various non-hydrolyzable C–C– and C–O– bonds (6). For many years, it was thought that only the ligninolytic system of some white-rot fungi capable of degrading this recalcitrant polymer to a major extent involved lignin peroxidase and manganese peroxidase (7). Although the latter can only oxidize the phenolic components of lignin, lignin peroxidase, which has a high redox potential, is also capable of cleaving the non-phenolic aromatic bonds. Since laccase alone is incapable of cleaving the non-phenolic bonds of lignin, it was not considered a significant component of the ligninolytic system, despite the secretion of large quantities of laccase by these fungi under ligninolytic conditions. However, Bourbonnais and Paice (8) reported that laccases can catalyze the oxidation of non-phenolic benzylalcohols in the presence of a mediator, such as 2,2′-azino-bis-[3-ethylthiazoline-6-sulfonate]. This finding led to the discovery that laccase-mediator systems effectively degrade residual lignin in unbleached pulp (9). Furthermore, laccases produced by some wood-rotting fungi from the genus *Basidiomyete* do in fact play a major role in the biodegradation of lignin (10) and have the capability to oxidize recalcitrant aromatic compounds with redox potentials exceeding their own (2). This ability has been exploited in various industrial processes such as pulp deligni-

* This work was supported in part by grants from the SNF (Swiss National Science Foundation, Grant No. 31-55681.98) and the BBW (Swiss Ministry of Education and Science, BBW No. 99.0585) (to K. P.). The latter grant belongs to a project within the 5th European Framework Programme (PELAS, QLK 3 1999 590). The costs of publication of this article were defrayed in part by the payment of page charges. This article must therefore be hereby marked "*advertisement*" in accordance with 18 U.S.C. Section 1734 solely to indicate this fact.

The atomic coordinates and structure factors (code 1GYC) have been deposited in the Protein Data Bank, Research Collaboratory for Structural Bioinformatics, Rutgers University, New Brunswick, NJ (http://www.rcsb.org/).

‡ To whom correspondence should be addressed. Tel.: 41-1-632-3141; Fax: 41-1-632-1121; E-mail: klaus.piontek@bc.biol.ethz.ch.

§ Most of this research was part of a Ph.D. thesis (35).

[1] The abbreviations used are: bmCuO, blue multicopper oxidase; AO, ascorbate oxidase; CcL, *C. cinereus* laccase; E^0, redox potential; T1, type-1; T2, type-2; T3, type-3; TvL, *T. versicolor* laccase.

fication (11) and bioremediation of soils and water (12), and this area of research is the subject of intense biotechnological activity.

A question that is yet to be answered is to ascertain how these different bmCuOs modulate their redox potentials (E^0) (13) at the structural level, despite having very similar (14) or seemingly equal copper coordination geometry (15). Investigations into this issue are especially relevant in the case of the laccases (15–17) because they cover such a wide range of E^0s. This has led to their classification as low (500 mV *versus* normal hydrogen electrode) and high (700–800 mV) E^0 laccases (15) and has important implications for their biotechnological application and future manipulation of this property by protein engineering strategies.

Crystal structures of AO (18) and mammalian plasma ceruloplasmin (19) were determined some years ago, but despite being an enzyme that referred to many questions regarding the catalytic mechanism in bmCuOs and despite being the smallest representative of the bmCuO family, no structure of an active laccase is presently available. Ducros *et al.* (20) reported the crystal structure of a laccase from the fungus *Coprinus cinereus*. This was found to be a copper type-2-depleted form in which the putative T2 copper is completely absent and therefore is in a catalytically incompetent state. The difficulties in successfully crystallizing the active form of laccase have been unanimously attributed to the occurrence of extensive microheterogeneity, presumably caused by variable glycosylation of the enzyme. Unfortunately, deglycosylation to obtain high quality diffracting crystals of the *C. cinereus* laccase (CcL) resulted in the loss of copper.

Recently, we reported the purification of laccase isozymes from the fungi *Trametes versicolor* and *Pycnoporus cinnabarinus* to apparent isoelectric homogeneity without deglycosylation (21). These protein samples were fully active, and crystals obtained diffracted to high resolution (21). We now report the crystal structure of a *T. versicolor* laccase (TvL) in its oxidized, copper-complete state. This structure gives the first insight into the coordination of all the four copper centers in the fully active enzyme. Our structural data suggest a mechanism, which we support with comparative sequence data, by which laccases could tune their redox potential.

EXPERIMENTAL PROCEDURES

Protein Purification, Crystallization, and X-ray Data Collection—Laccase isozymes from *T. versicolor* (ATCC 20869) were obtained from fungal cultures grown in medium prepared as described (22). One of the TvL isozymes could be purified to apparent isoelectrophoretic homogeneity and was used for subsequent crystallization experiments. Crystallization, data collection, synchrotron radiation, and processing were reported previously (21). In brief, orthorhombic crystals of space group $P2_12_12_1$ were obtained with 20% polyethylene glycol 8000, 20% isopropanol, 100 mM sodium citrate, pH 5.6. Cell dimensions are a = 83.6 Å, b = 85.0 Å, c = 91.5 Å with a corresponding V_m of 2.3 Å^3/Da, assuming one molecule per asymmetric unit. The activity of redissolved crystals was tested with a standard assay and showed full activity, verifying that no copper loss took place. Even after exposure to x-rays, most of the activity of the enzyme in the crystal was maintained. Diffraction data were collected at the European Molecular Biology Laboratory (EMBL) beamline BW7B of the synchrotron Deutsches Elektronen Synchrotron (DESY)/Hamburg at room temperature. The data were processed and scaled with the programs DENZO and SCALEPACK of the HKL suite (23). For the 1.9–20-Å resolution shell, the data are 99.7% complete and scale with an overall R_{sym} of 0.063 and with an R_{sym} of 0.38 for the data in the highest resolution shell (1.97–1.90 Å).

Structure Solution and Refinement—For the structure determination, the molecular replacement technique was applied using the structure of CcL (Protein Data Bank code 1A65) as the search model. Water molecules and copper atoms were omitted from the model. Side chains of non-identical amino acid types (29%) were trimmed to alanines or glycines, as appropriate. This model was then used within the program AMoRe (24) to calculate cross-rotation and translation functions in the 10–4-Å resolution range. The correct solution corresponded to the highest peak in the cross-rotation and translation function, being well discriminated from the next highest peak. After rigid body refinement with 10–2.5 Å resolution data, an R_{cryst} of 0.434 was obtained. A $2F_o - F_c$ electron density map revealed clearly all four copper sites. Difference maps, including omit maps calculated with the method described by Bhat (25), allowed initial model building of most of the polypeptide chain. Repeated rounds of model building and maximum likelihood refinement with REFMAC resulted finally in a complete and well defined model with an R_{work} = 0.168 for all data of between 20 and 1.9-Å resolution and with a good stereochemistry (Table I). Only 3 out of the total 499 amino acids are in the generously allowed region of a Ramachandran plot. Since the protein was isolated from fungal culture medium, a major concern was to characterize the enzyme in terms of its primary sequence. The sequence of the first 20 N-terminal amino acids was determined by Edman degradation and was compared with the available laccase gene sequences from *T. versicolor*. The best agreement was with an N-terminal peptide of *T. versicolor* laccase I, encoded by the lac2 precursor gene sequence, as deposited with the Swiss Protein Database under code Q12718 (www.expasy.ch). In addition since this is the only available sequence with an arginine at position 43 and the electron density clearly indicates such a side chain (see Fig. 1*a*), this gene sequence was used for model building. All programs not explicitly mentioned were part of the CCP4 package (26). Model building was performed with the programs *O* (27) and CHAIN (28). MOLSCRIPT (29)/RASTER3D (30), and GRASP (31) were used to produce ribbon diagrams, electrostatic surface potential plots, and electron density representations.

TABLE I
Refinement statistics of TvL

Resolution range (Å)[a]	20–1.9 (2.02–1.90)
R_{work}/R_{free}[b]	16.8 (21.0)/20.9 (25.7)
Total no. of atoms	4,356
No. of water molecules	449
Mean B-factors (Å^2)	26.2
Protein	23.5
Carbohydrates	41.9
Water molecules	45.5
Copper cations	21.8
Deviations from ideal geometry (Å)	
Bonds	0.011
Angles	0.026

[a] Values for the highest shell in parentheses.
[b] R_{free} calculated with 5% of the data.

TABLE II
Amino acids of the gene sequence LccI (Swiss Protein Database accession code Q12718), which do not fit to the electron density of the TvL crystal structure

Gene sequence	X-ray sequence
Val-5	Ala-5
Val-31	Phe-31
Asp-49	Val-49
Ser-56	Thr-56
Val-259	Ile-259
Asp-460	Glu-460

RESULTS

Overall Structure—The laccase from the ligninolytic fungus *Trametes versicolor* could be crystallized, and the structure of the fully active enzyme was determined. An excellent electron density allowed the modeling of the complete polypeptide, all four copper ions, and a total of seven *N*-acetyl glucoseamine moieties at five distinct *N*-glycosylation sites (see Fig. 2). The protein appears to correspond to the sequence encoded by the gene LccI (32), despite a few inconsistencies. In total, 6 amino acids of this gene sequence do not fit to the crystal structure (Table II). Since the corresponding electron densities are of a very good quality (Fig. 1), which allows an unambiguous identification of the side chains, we have to assume gene sequencing errors, the occurrence of multiple alleles, or the presence of an as yet unreported gene sequence.

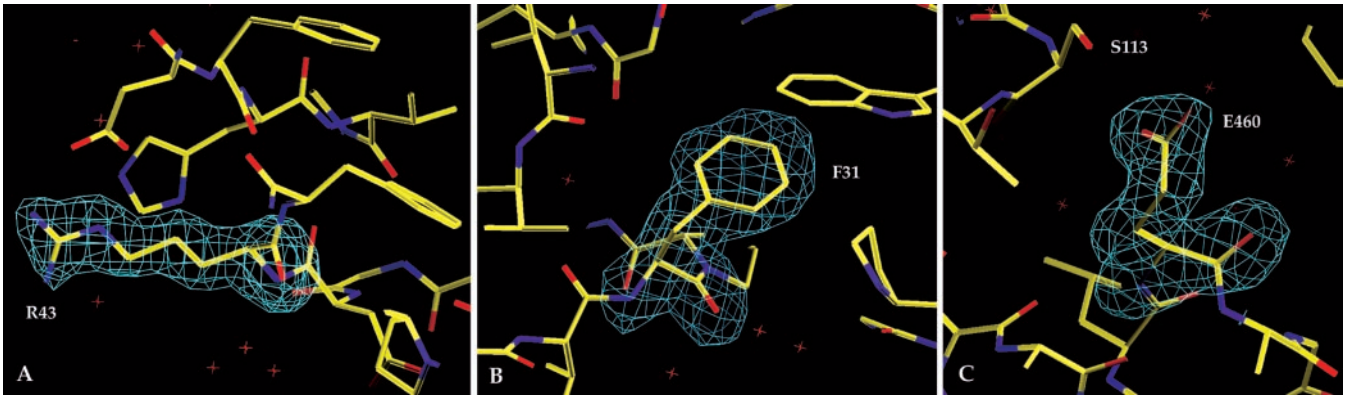

FIG. 1. **Difference electron density maps of amino acids, which were critical for the assignment of the gene sequence to the crystal structure of TvL.** For the calculation of the coefficients $(F_o - F_c)\exp(i\alpha_c)$, the phase contribution of the respective residue was omitted. The maps are contoured at 3.2 σ levels. The used sequence is the only one in which an arginine is present at position 43 (*A*). According to the gene sequence, residue 31 is reported to be a valine (see also Table II). The electron density clearly indicates a phenylalanine in this position (*B*). According to the gene sequence, residue 460 is reported to be an aspartate (see also Table II, and see "Results" and "Discussion" for further discussion of Glu-460). The electron density clearly indicates a glutamate in this position (*C*).

The TvL structure is a monomer, organized in three sequentially arranged domains (Fig. 2), and has dimensions of about $65 \times 55 \times 45$ Å^3. Each of the three domains is of a similar β-barrel type architecture, related to the small blue copper proteins such as azurin or plastocyanin. Domain 1 comprises two four-stranded β-sheets and four 3_{10}-helices. Three of the 3_{10}-helices are in connecting peptides between the β-strands, and one is in a segment between domain 1 and 2. The second domain has one six-stranded and one five-stranded β-sheet, and like in domain 1, there are three 3_{10}-helixes in peptides connecting individual β-strands and domains 1 and 3, respectively. A 3_{10}-helix between domains 2 and 3 forms part of a 40-residue-long extended loop region. Finally, domain 3 consists of a β-barrel formed by two five-stranded β-sheets and a two-stranded β-sheet that, together with an α-helix and a β-turn, form the cavity in which the type-1 copper is located. The tri-nuclear copper cluster (T2/T3) is embedded between domains 1 and 3 with both domains providing residues for the coordination of the coppers. The third domain has the highest helical content with one 3_{10}-helix and two α-helices located in the connecting regions between the strands of the different β-sheets. Finally, at the C-terminal end of domain 3, three sequentially arranged α-helices complete the fold. A 13-amino-acid-long α-helix at the C-terminal portion is stabilized by a disulfide bridge to domain 1 (Cys-85–Cys-488), and a second disulfide bridge (Cys-117–Cys-205) connects domains 1 and 2. Both N-terminal and C-terminal amino acids benefit from hydrogen bonding networks to the rest of the protein, providing sufficient rigidity so that excellent electron density can be observed for these regions in the crystal structure (Fig. 3). A comparison of individual domains with other known structures of the blue copper proteins shows that they have essentially the same topology. However, TvL is most similar to CcL (Table III), as was anticipated from the close sequence relationship and from the results of the molecular replacement experiments, despite the lack of the T2 copper site in CcL.

The electrostatic surface potential distribution of TvL reveals a dominance of negative charges, which is in accordance with the acidic pI of about 3.5. From the crystal structure of an enzyme/substrate complex,[2] we know that the substrate binds in a small negatively charged cavity near the copper T1 site. The negative charges located at this site may have functional significance since they could stabilize the radical cation products that are formed during the catalytic cycle.

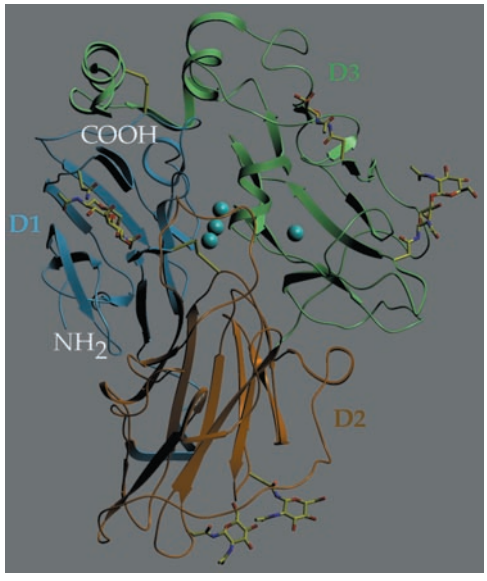

FIG. 2. **Ribbon diagram of TvL.** The arrangement of the domain structure is depicted in different *color coding* (D1–D3). Copper ions are drawn as *blue spheres*. Carbohydrates and disulfide bonds are included as *stick models*.

The oxygen-reducing site at the T2/T3 cluster has access to solvent through two channels, which lead to the type-3 copper sites and to the type-2 copper site, respectively (Fig. 4). The latter site is more exposed and more labile as compared with the other two at the T3 site. In fact, it is the T2 copper site that is deficient in copper in the copper-depleted forms of both laccase and ascorbate oxidase (20, 33). Water molecules found in the two channels are well defined in the electron density and form numerous hydrogen bonds with the surrounding residues. Superposition of TvL with CcL and AO (Protein Data Bank code 1AOZ) shows that these water molecules and the amino acids that form the channels are highly conserved. A "two-site ping-pong bi-bi" reaction mechanism has been proposed for laccase (34), which means that products are released before binding of new substrates occurs. It appears that the solvent channels of the blue copper oxidases are well suited to allow fast access of dioxygen molecules to the trinuclear cluster and subsequently easy release of water.

Copper Coordination—Using unitary occupancies, the B-factors of the copper cations refined to a mean value of 21.3 Å^2

[2] K. Piontek, M. Antorini, and T. Choinowski, unpublished observation.

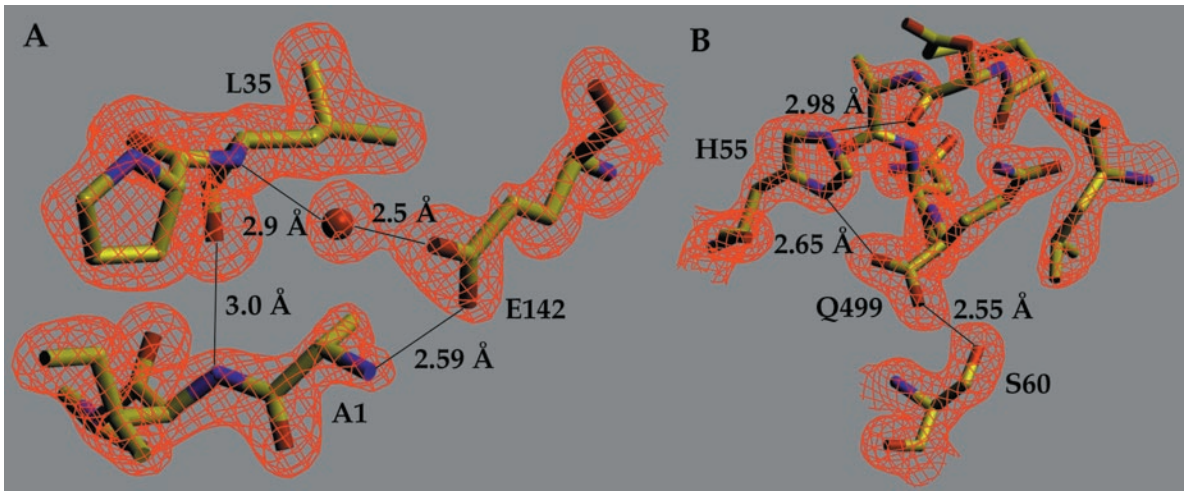

FIG. 3. **Electron density of TvL around the N terminus (*A*) and C terminus (*B*).** The two maps are calculated with $(2F_o - F_c)\exp(i\alpha_c)$ coefficients and are contoured at 1.8-σ levels. *Thin lines* represent the hydrogen-bonding network by which residues Ala-1 and Gln-499 are stabilized.

TABLE III
Root mean square deviation (Å) of Cα-atoms from the superposition of TvL domains with equivalent domains of CcL and AO and with azurin and plastocyanin

	D1_TvL	D2_TvL	D3_TvL
D1_CcL	0.97		
D2_CcL		0.96	
D3_CcL			0.76
D1_AO	1.05		
D2_AO		1.18	
D3_AO			1.21
Azurin	1.29	1.52	1.21
Plastocyanin	1.69	1.50	1.69

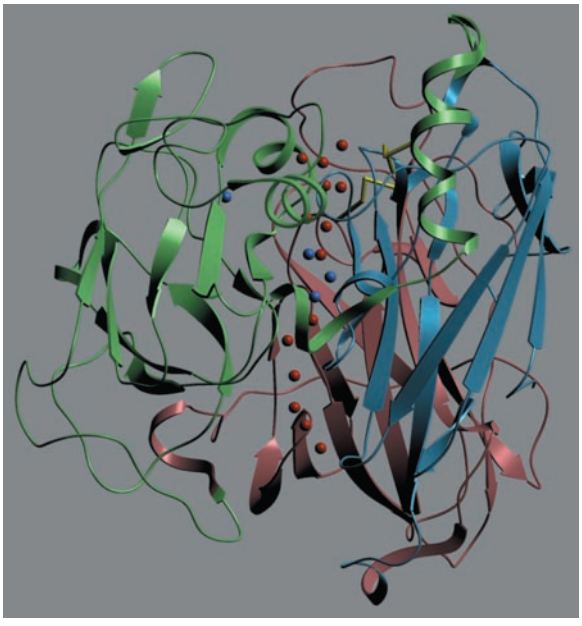

FIG. 4. **Ribbon diagram of TvL showing the two channels leading to the T2/T3 cluster.** Water molecules are depicted as *red spheres*, and copper ions are depicted as *blue spheres*.

(17.5–24.4. Å^2). This is significantly lower than the average value of all atoms in the crystal structure (26.2 Å^2). Since the mean temperature factor of all amino acids is 23.4 Å^2, we assume that the copper sites are fully occupied.

The trinuclear copper center of TvL is situated between domains 1 and 3 and is buried about 12 Å deep within the molecule. The three coppers are arranged in an almost perfect regular triangle with a mean distance of 3.85 Å (Fig. 5). Cu2 and Cu3 of the T3 site are 3.9 Å apart, whereas the distances of these two coppers to the T2 copper (Cu4) are 3.8 Å each. In between the two T3 coppers, there is an oxygen ligand, either a OH^- or O^{2-} molecule, that coordinates with the Cu2 and Cu3. This gives bond lengths of 2.19 and 2.08 Å, respectively, with an angle of 133°. A total of six histidines coordinate to the two T3 coppers in a symmetrical way with a mean distance of 2.16 Å. Therefore, the ligation of each of these coppers is 4-fold, and their coordination sphere can be best described as being distorted tetrahedral. Five of these histidines supply their Nϵ2 atoms and one its Nδ1 atom. The T2 copper has two Nϵ2 ligands from two histidines and one oxygen ligand, forming a trigonal coplanar configuration. The exact character of the oxygen ligand could not be determined from the crystal structure, as is also the case for the bridging ligand of the T3 coppers, but it is either a water or OH^- molecule. The geometry of the T2/T3 cluster is very similar to the one found in the crystal structure of AO (19). In fact, the corresponding Cu–Cu and Cu–N/O bond lengths deviate only slightly, although there is a noticeable tendency for longer bond distances in the case of TvL. A comparison of the trinuclear copper cluster with the one of CcL (21) is not appropriate. This is mainly because there is no T2 copper in the crystal structure of CcL and because copper depletion has profound effects on the coordination of the T3 copper atoms. For CcL, one of the putative histidine ligands coordinates to the Cu2 of the T3 site, making this copper penta-coordinated, with four histidine ligands and the bridging ligand. The latter is now asymmetrically positioned between the two coppers, being 2.1 Å away from Cu2 but 3.1 Å away from Cu3, which should not be considered a bonding distance, and therefore, the oxygen is not a bridging ligand in the CcL structure. The two coppers are now 4.9 Å apart, roughly 1 Å more than in TvL and AO, whereas the Cu3 atom is in a trigonal planar coordination.

The mononuclear copper of the T1 center lies embedded in domain 3, about 6.5 Å below the surface of the enzyme. The copper occupies a depression of the enzyme surface, delimited by a β-turn, belonging to domain 1, and two β-turns of domain 3, which are involved in substrate binding. It is therefore reasonable to assume that the T1 copper is the primary electron acceptor site. The T1 copper is connected to the trinuclear cluster by a His-Cys-His tripeptide, which is highly conserved among bmCuOs. The closest distance between the T1 and T2/3

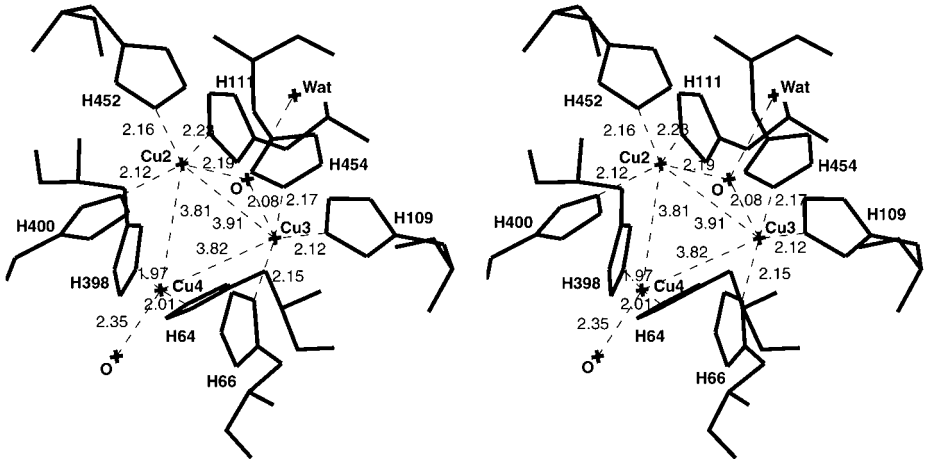

FIG. 5. **Stereo view of the T2/T3 coppers and their close environment in TvL.** Bonds are represented by *thin*, *dashed lines*, and lengths are given in Å.

coppers is about 12 Å. Theoretical electron transfer pathways have been calculated for AO (1). Due to the high similarity with laccase, similar inferences can be drawn here for TvL. The most favored pathway is predicted from the sulfur of the Cu1-ligating cysteine to its carbonyl oxygen and then via a hydrogen bond to the Nδ1 of His-452, which coordinates to Cu2 of the T3 site. In the TvL structure, the T1 copper is unlike in the classical blue centers trigonal coplanar coordinated. The ligands are supplied by a sulfur atom of a cysteine and by the Nδ1 nitrogen of two histidines (Fig. 6). Usually, type-1 centers have a sulfur from a methionine as an additional axial ligand. In the case of TvL, there is a phenylalanine in this position. The latter has a distance of 3.6 Å from the copper and does not participate in the coordination. As a consequence of this arrangement, the copper ion lies practically within the plane formed by the two nitrogen and one sulfur ligands, whereas in the case of copper proteins possessing an additional axial ligand, the copper lies above the plane toward the sulfur ligand. Thus, the coordination of the T1 copper in TvL is different from the ones found in, for example, AO, azurin, and plastocyanin, which supply an additional axial ligand. The situation is comparable with the T1 copper site of CcL, which has a leucine in the position of the potential axial ligand and obviously cannot coordinate the copper as well. Comparison of the Cu–N/S distances shows that they are similar in both fungal laccase structures (Table IV), although they appear somewhat longer in TvL. The significance of these differences, albeit small, is discussed below.

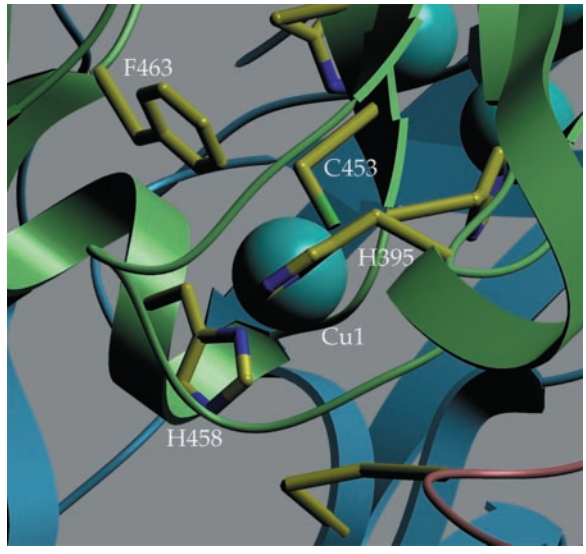

FIG. 6. **Close-up view into the T1 site of TvL.** The copper is depicted as a *large sphere*, and the protein backbone is depicted as a *ribbon*. For clarity, only the copper-ligating amino acids and the residue (Phe-463) in the axial position are shown in *stick representation*.

TABLE IV
Copper-ligand distances (Å) of the T1 site in TvL and CcL

	TvL	CcL
Cu1-Nδ1 (His-395)	2.02	1.91
Cu1-Nδ1 (His-458)	2.04	1.87
Cu1-Sγ (Cys-453)	2.19	2.27

DISCUSSION

The first crystal structure of an active laccase containing a full complement of coppers has been determined to high resolution. We solely attribute the success of obtaining good diffracting crystals to the preparation of an isozyme sample to apparent isoelectrophoretic homogeneity. This structure allows a detailed insight into the geometry of the four copper sites in the intact enzyme in this, the smallest of the family of blue multicopper oxidases.

A comparison of the trinuclear cluster and its environment in TvL with that of other known structures of this enzyme family shows that it is structurally highly conserved. This is true for the copper geometry, for the two channels, which provide access for molecular oxygen to and release of water from the T2/T3 cluster, as well as for the conserved His-Cys-His tripeptide, implicated in the electron transfer pathway between the T1 copper and the trinuclear cluster. This structural conservation reflects a common reaction mechanism for the copper oxidation and the O_2 reduction in these enzymes. Interestingly, reoxidation of the coppers occurs at exactly the same rate of 5×10^6 M^{-1} sec^{-1} in both laccase and AO (36, 37).

Different is the situation concerning the specificity for and reactivity toward reducing substrates in the blue multicopper oxidases. Substrate specificity is usually defined by the geometry and chemical nature of the substrate binding pocket. Such a pocket or crevice provides a suitable environment for the binding of the substrate(s) and their emerging intermediates. In a follow-up report, based on the crystal structure of a substrate complex of TvL, this issue will be discussed in detail. Concerning the reactivity of TvL, in comparison with other laccases and bmCuOs, the discussion will now continue on the T1 copper ligation and its possible effect on the redox potential. The reactivity of laccases has been correlated by some authors with their redox potential (3) and is thought to play a major role in the overall performance of an enzyme.

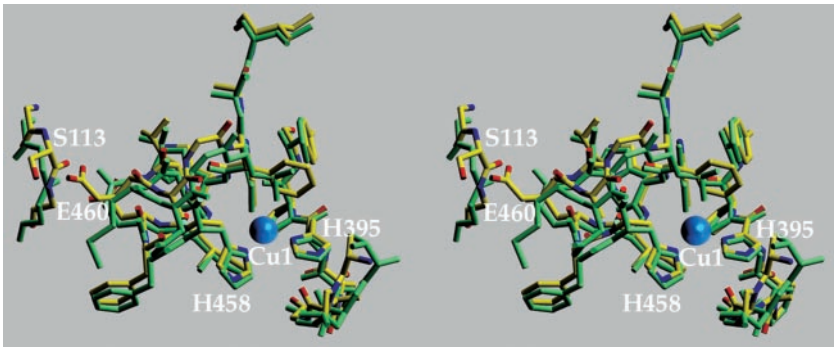

FIG. 7. **Stereo view of a superposition of CcL onto TvL at the T1 copper showing the surrounding residues and a peptide containing Ser-113.** TvL is depicted in *atomic color coding*, and CcL is depicted in *green*. The root mean square deviation of the Cα-atoms of residues 458 and 460 are 0.54 and 0.78 Å, respectively. Note that in the peptide containing the second T1 copper-ligating histidine (His-395), equivalent atoms of the two laccase structures are significantly closer, which correlates with the smaller difference of the two Cu1–N (His-395) bonds as compared with the situation of the Cu1–N (His-458) bond (see also Table IV).

Contrary to other blue copper oxidases, the coordination of the T1 copper in TvL and CcL is trigonal coplanar. The typical coordination of type-1 coppers in bmCuOs and in the small copper enzymes consists of two histidines, one cysteine, and one axial methionine and is therefore 4-fold. Axial coordination has been considered to be one factor affecting the redox potential of copper enzymes (38, 39). Mutational studies on azurin showed that the substitution of methionine by a leucine resulted in an increase of the E^0 by about 0.1 V (40). In CcL, which has a redox potential of 550 mV, the axial position is occupied by a leucine, whereas in TvL, with a redox potential of 800 mV, there is a phenylalanine in the corresponding position. Thus, it has been speculated that a phenylalanine in the axial position is responsible for the very high E^0 of TvL. However, *Neurospora crassa* laccase with a leucine in the axial position also has a high E^0 of 780 mV. Furthermore, by mutagenesis studies, it was demonstrated that a Leu-Phe mutation of this axial residue had virtually no influence on the redox potential (15). All these data suggest that other factors are more important.

With the structure determination of TvL, structural information is now available of a high E^0 laccase, which can be compared with the structure of the low E^0 enzyme from *C. cinereus*, to explain the structural origin of the difference in redox potential. We noticed that the Cu1-Nδ2 (His-458) distance in TvL is 0.17 Å longer than in CcL, which is the most noticeable difference at the T1 copper site (Table IV). An elongated Cu–N bond could have an effect on the redox potential since the contribution of the free electron pair from the nitrogen to the copper would be decreased, rendering the copper more electron deficient. This would give rise to a destabilization of the higher oxidation states. In other words, the copper redox potential should increase. Consequently, we searched for structural components, which could cause the longer Cu–N bond and which could also be found in other high E^0 laccases. Superposition of the two structures revealed that a small α-helix (residues 455–461), which carries the copper T1 ligating His-458 in TvL, is displaced away from the copper, as compared with its corresponding position in CcL (Fig. 7). A hydrogen bond between Glu-460 and Ser-113, the latter being situated in the opposite domain 1 (Fig. 8), seems to be responsible for this. Interestingly, this particular serine is one of the three residues in the generously allowed region of the Ramachandran plot. It is presumably forced by the hydrogen bond into an unfavorable main chain conformation. As a consequence of the attractive H-bond interaction, the whole helix, which contains His-458, is pulled toward domain 1, thus increasing the Cu–N distance (Fig. 8). In CcL, the position of the Glu-460 is taken by a methionine that cannot form such a hydrogen bond. Moreover,

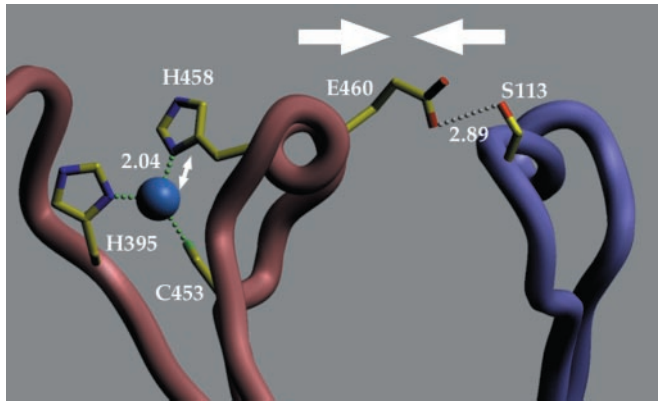

FIG. 8. **Schematic drawing illustrating the movement of a helical segment in TvL.** Upon formation of a hydrogen bond between Glu-460 and Ser-113, a movement of the helical segment carrying His-458 could result, which would subsequently cause an elongation of the Cu1-N (His-458) bond at the T1 site. In low E^0 laccases, such a hydrogen bond is not possible, due to the lack of an appropriate hydrogen bond donor and acceptor. The bond lengths are given in Angstroms.

the position corresponding to Ser-113 is a glycine in CcL. It might be argued that the difference in the Cu–N bond lengths is statistically not meaningful since an estimate of the coordinate error calculated with the method described by Luzatti (41) gives a value of 0.16 Å. As pointed out by Baker (42), this estimate indicates a maximum coordinate error. The copper atoms and their neighboring protein residues are among the best defined atoms in the whole crystal structure with low temperature factors. It is therefore most probable that their coordinate errors are lower than the value given above. Even if one assumes a significantly lower coordinate error for the coppers and their ligands in TvL, the coordinate error of the CcL crystal structure has to be taken into account. Although this value has not been reported, based on the R-factor and the resolution, an error of about 0.15–0.20 Å would be realistic. Therefore, based on statistical grounds, a definitive statement on the reliability of the different Cu–N bond lengths (for the copper type-1) cannot be given. However, the mechanism suggested above and its possible effect on the redox potential is supported by the structural evidence (the presence of the Ser-Glu hydrogen bond) and in particular by a comparison of the available sequences and their correlation with known redox potentials of laccases. These sequence data reveal that a glutamic acid in the position corresponding to Glu-460 and a serine corresponding to Ser-113 in TvL is a highly conserved feature among high E^0 enzymes, as well as in some laccases of ligninolytic fungi with unknown E^0. We would assume that the

latter most likely are also high E^0 enzymes.

Previously, a Leu-Glu-Ala tripeptide, immediately following the copper ligating His-458, has been assumed to be characteristic for the high E^0 laccases (15). The glutamate in this peptide corresponds to the aforementioned Glu-460 in TvL. Moreover, TvL has such a Leu-Glu-Ala sequence, typical for the high E^0 laccases, whereas CcL has Leu-Met-Asn in the equivalent position. In an attempt to tune the redox potential of recombinant laccases, the high E^0 sequence was inserted into low E^0 enzymes and *vice versa* (15). Although marginal changes in the phenol-oxidase activity were observed, which could be explained by the fact that this peptide is part of the substrate binding pocket, the redox potential was not affected. The lack of an appropriate counterpart in these studies, being equivalent to Ser-113, could explain why these studies were unsuccessful in increasing the redox potential of the low E^0 form.

It has been demonstrated previously that an axial methionine ligand at the T1 copper is responsible for a change in the redox potential of about 100 mV. Additional structural determinants, which could be utilized by blue copper oxidases to tune the potential over a larger range, have been lacking so far. Based on our structural data, we suggest a new mechanism by which laccases and possibly also other redox metallo-enzymes, can increase their redox potential by more than 200 mV. Such a mechanism assumes a lessening of electron density contribution at the metal cation through a stretching of the bond between the metal and the ligating amino acid. This movement could be caused by an appropriate hydrogen bond that results in the displacement of the polypeptide segment, which carries the coordinating amino acid. Our laboratory is currently involved in site-directed mutagenesis studies to test this proposition and to provide possibly a definitive answer to this intriguing question.

Acknowledgments—We gratefully acknowledge the opportunity to collect diffraction data at the European Molecular Biology Laboratory Outstation (Deutsches Elektronen Synchrotron (DESY)/Hamburg) and at the Swiss Norwegian Beamline (European Synchrotron Radiation Facility/Grenoble). We thank Dr. Gideon J. Davies, University of Heslington, York, UK, for providing the coordinates of CcL prior to public release and Dr. Andrew T. Smith, University of Sussex, Brighton, UK, for carefully reading the manuscript.

REFERENCES

1. Messerschmidt, A. (ed) (1997) *Multi-copper Oxidases*, World Scientific, Singapore
2. Xu, F. (1996) *Biochemistry* **35,** 7608–7614
3. Xu, F., Shin, W., Brown, S. H., Wahleithner, J. A., Sundaram, U. M. & Solomon, E. I. (1996) *Biochim. Biophys. Acta* **1292,** 303–311
4. Sakurai, T. (1992) *Biochem. J.* **284,** 681–685
5. Yoshida, H. (1883) *J. Chem. Soc.* (Tokyo) **43,** 472–486
6. Gellerstedt, G. & Northy, R. A. (1989) *Wood Sci. Technol.* **23,** 75–83
7. Evans, C. S. (1985) *FEMS Microbiol. Lett.* **27,** 339–343
8. Bourbonnais, R. & Paice, M. G. (1990) *FEBS Lett.* **267,** 99–102
9. Call, H. P. (December 22, 1994) World Patent Application WO 94/29510
10. Coll, P. M., Fernandez-Abalos, J. M., Villanueva, J. R., Santamaria, R. & Perez, P. (1993) *Appl. Environ. Microbiol.* **59,** 2607–2613
11. Sealey, J. & Ragauskas, A. J. (1998) *Enzyme Microb. Technol.* **23,** 422–426
12. Li, K., Xu, F. & Eriksson, K.-H. L. (1999) *Appl. Environ. Microbiol.* **65,** 2654–2660
13. Fee, J. A. & Malmström, B. G. (1968) *Biochim. Biophys. Acta* **153,** 299–302
14. Hough, M. A., Hall, J. F., Kanbi, L. D. & Hasnain, S. S. (2001) *Acta Crystallogr. Sect. D Biol. Crystallogr.* **57,** 355–360
15. Xu, F., Berka, R. M., Wahleithner, J. A., Nelson, B. A., Shuster, J. R., Brown, S. H., Palmer, A. E. & Solomon, E. I. (1998) *Biochem. J.* **334,** 63–70
16. Xu, F., Kulys, J. J., Duke, K., Li, K., Krikstopaitis, K., Deussen, H.-J. W., Abbate, E., Galintye, V. & Schneider, P. (2000) *Appl. Environ. Microbiol.* **66,** 2052–2056
17. Xu, F., Palmer, A. E., Yaver, D. S., Berka, R. M., Gambetta, G. A., Brown, S. H. & Solomon, E. I. (1999) *J. Biol. Chem.* **274,** 12372–12375
18. Messerschmidt, A., Ladenstein, R., Huber, R., Bolognesi, M., Avigliano, L., Petruzzelli, R., Rossi, A. & Finazzi-Agro, A. (1992) *J. Mol. Biol.* **224,** 179–205
19. Zaitseva, I., Zaitsev, V., Card, G., Moshkov, K., Bax, B., Ralph, A. & Lindley, P. (1996) *J. Biol. Inorg. Chem.* **1,** 15–23
20. Ducros, V., Brzozowski, A. M., Wilson, K. S., Brown, S. H., Østergaard, P., Schneider, P., Yaver, D. S., Pedersen, A. H. & Davies, G. J. (1998) *Nat. Struct. Biol.* **5,** 310–316
21. Antorini, M., Herpoël-Gimbert, I, Choinowski T., Asther, M., Sigoillot, J. C., Winterhalter, K. H. & Piontek, K. (2002) *Biochim. Biophys. Acta* **1594,** 109–114
22. Fahraeus, G. & Reinhammar B. (1967) *Acta Chem. Scand.* **21,** 2367–2378
23. Otwinowski, Z. & Minor, W. (1997) *Methods Enzymol.* **276,** 307–326
24. Navaza, J. (2001) *Acta Crystallogr. Sect. D Biol. Crystallogr.* **57,** 1367–1372
25. Bhat, T. N. (1988) *J. Appl. Crystallogr.* **21,** 279–281
26. Collaborative Computing Project, Number 4 (1994) *Acta Crystallogr. Sect. D Biol. Crystallogr.* **50,** 760–763
27. Jones, T. A., Zou, J.-Y., Cowan, S. W. & Kjeldgaard, M. (1991) *Acta Crystallogr. Sect. A* **47,** 110–119
28. Sack, J. S. (1988) *J. Mol. Graph.* **6,** 224–225
29. Kraulis, P. J. (1991) *J. Appl. Crystallogr.* **24,** 946–950
30. Merritt, E. A. & Bacon, D. J. (1997) *Methods Enzymol.* **277,** 505–524
31. Nicholls, A., Sharp, K. & Honig, B. (1991) *Proteins* **11,** 281–296
32. Ong, E., Pollock, W. B. & Smith, M. (1997) *Gene* (*Amst.*) **196,** 113–119
33. Messerschmidt, A., Steigemann, W., Huber, R., Lang, G. & Kroneck, P. M. (1992) *Eur. J. Biochem.* **209,** 597–602
34. Petersen, L. C. & Degn, H. (1978) *Biochim. Biophys. Acta* **526,** 85–92
35. Antorini, M. (2000) *Structural and functional analysis of a laccase from the ligninolytic fungus Trametes versicolor*. Ph.D. thesis, ETH Zürich, Switzerland, Diss. ETH No. 13818
36. Andreasson, L.-E., Bränden, R. & Reinhammar, B. (1976) *Biochim. Biophys. Acta* **438,** 370–379
37. Nakamura, T. & Ogawa, Y. (1968) *J. Biochem.* (Tokyo) **64,** 267
38. Machonkin, T. E., Quintanar, L., Palmer, A. E., Hassett, R., Severance, S., Kosman, D. J. & Solomon E. I. (2001) *J. Am. Chem. Soc.* **123,** 5507–5517
39. Malmström, B. G., Reinhammar, B. & Vanngard, T. (1970) *Biochim. Biophys. Acta* **205,** 48–57
40. Farver, O., Skov, L. K., Pascher, T., Karlsson, B. G., Nordling, M., Lundberg, L. G., Vanngard, T. & Pecht, I. (1993) *Biochemistry* **32,** 7317–7322
41. Luzatti, P. V. (1952) *Acta Crystallogr.* **5,** 802–810
42. Baker, E. N. (1988) *J. Mol. Biol.* **203,** 1071–1095

Crystal Structure of a Laccase from the Fungus *Trametes versicolor* at 1.90-Å Resolution Containing a Full Complement of Coppers

Klaus Piontek, Matteo Antorini and Thomas Choinowski

J. Biol. Chem. 2002, 277:37663-37669.